EXPERIMENTAL STUDY ON MECHANICAL PERFORMANCES OF DIFFERENT FIBRE REINFORCED LIGHTWEIGHT CONCRETES

XIAOGANG WU[1], SHUREN WANG[1,2] * , JIANHUI YANG[3], SEN ZHU[3]

[1] *International Joint Research Laboratory of Henan Province for Underground Space Development and Disaster Prevention, Henan Polytechnic University, Jiaozuo 454003, China*

[2] *School of Minerals and Energy Resources Engineering, University of New South Wales, Sydney, NSW 2052, Australia*

[3] *Henan Province Engineering Laboratory for Eco-architecture and the Built Environment, Henan Polytechnic University, Jiaozuo 454003, China*

In view of the significant influence of fibre type and dosage on the mechanical properties of lightweight concrete, an experimental study was undertaken to analyze the mechanical performance characteristics, including compressive strength, splitting tensile strength, energy absorption, high temperature deterioration performance, fracture toughness and dynamic mechanical properties of steel fibre reinforced all lightweight concrete (SFRALWC), polypropylene fibre reinforced all lightweight concrete (PFRALWC), and basalt fibre reinforced all lightweight concrete (BFRALWC). Results showed that the specific strength, energy absorption index and dynamic peak stress of shale ALWC/FRALWC improved with the increase of the compressive strength, and the relation exhibites strong correlation characteristics, which ccould be expressed by quadratic polynomial. SFRALWC with optimal fibre dosage had the highest splitting tensile strength, specific strength, compressive strength and fracture toughness values. Steel fibre (SF) could significantly increase the plasticity, high temperature resistance to deterioration and dynamic impact resistance of all lightweight concrete (ALWC). Polypropylene fibre (PPF) could improve the plasticity and inhibited the high temperature bursting performance of ALWC. BFRALWC was most sensitive to the strain rate of dynamic impact. The conclusions obtained in the study can provide the reference to the similar engineering.

Keywords: *Lightweight concrete, Fibre, Shale ceramsite, Dynamic impact, High temperature deterioration performance.*

1. Introduction

Ordinary concrete has obvious disadvantages, such as heavy weight and high brittleness, in engineering applications. High-strength, lightweight and multi-functional materials have become the direction of modern engineering. Lightweight concrete refers to concrete with a dry apparent density of no more than 1950 kg/m^3 formulated with lightweight aggregates. Compared with ordinary concrete of the same strength, the weight of lightweight concrete can be reduced by 20-25%, and it also has the advantages of heat preservation, earthquake resistance, sound insulation and impermeability [1,2]. The related studies showed that compressive strength, tensile strength, flexural strength and resistance to fatigue and impact could be improved by adding short fibres [3,4]. Therefore, fibre reinforced lightweight concrete has become a popular trend in the development of building materials and is widely used in long-span bridges, high-rise buildings, offshore platforms and other places where it is necessary to reduce the weight of the building materials, and it has good application prospects.

China has abundant resources of shale, and the production and application of shale lightweight concrete is very common. Concrete made from shale ceramsite as the coarse aggregate and shale sand as the fine aggregate, completely replacing gravel and sand, is called ALWC, with a density of only 1500-1700 kg/m^3 and compressive strength values up to 40 MPa. Compared with general lightweight concrete, the specific strength of ALWC was higher, which mean that the structure weight could be greatly reduced under the same strength grade conditions. The research on its material properties had received extensive attentions [5-7].

To improve the brittle fracture of ALWC, fibre reinforced lightweight concrete (FRALWC) was produced by the addition of steel fibres (SF), polypropylene fibres (PPF), basalt fibres (BF) and other fibres, and it exhibited excellent properties in many aspects, such as earthquake resistance and impact and crack resistance [8-10]. The development of concrete materials has entered the on-demand design stage and is no longer limited to the use of a single material. Different fibres have different specific functions and should be selected according to the requirements of the concrete design. Therefore, it is necessary to carry out experimental research on the mechanical properties of the SFALWC, PFALWC and BFALWC types commonly used in engineering.

2.State of the art

Lightweight aggregates are roughly composed of two types-natural (diatomaceous earth, pumice, volcanic ash, etc.) and man-made (expanded shale, perlite, clay, sintered PFA, slate, etc.). Lightweight concrete has the advantages of

* Autor corespondent/*Corresponding author*,
E-mail: w_sr88@163.com

low density, high relative strength, good heat preservation, good frost resistance, and low self-weight and has significant technical advantages. At present, a large number of experimental studies have revealed the mix proportion, strength-influencing factors and durability of lightweight concrete.

For examples, Babu et al. obtained expanded polystyrene concrete with a density of 1500-2000 kg/m^3 and a corresponding strength of 10-21 MPa by changing the silica fume content. They found that the 7-day compressive strength increased with the addition of silica fume content and that the durability of expanded polystyrene concrete was good [11]. Wang et al. improved the toughness of shale ceramsite concrete when waste rubber particles were added. They found that the bonding interface among rubber particles, shale ceramsite and cement slurry had a larger width, lower strength and greater toughness with increasing rubber particle content [12]. Zhuang et al. prepared lightweight concrete with pre-wet shale ceramsite for tensile creep experiments. They found that the pre-wet lightweight concrete had a lower creep value under the same conditions [13]. Zhang et al. studied the bond behaviour between bars and shale ceramsite lightweight aggregate concrete (SCLC) using pullout tests and obtained the load-slip relationship and failure modes [14].

Although the static mechanical properties of lightweight aggregate concrete have been extensively studied, most of these studies used lightweight concrete formed with lightweight coarse aggregates. There were few studies on the mechanical properties of ALWC prepared using shale ceramsite and shale sand. Wang et al. studied the static and dynamic mechanical properties of SFALWC. They found that the addition of steel fibres could greatly improve the splitting tensile strength, flexural strength, flexural toughness and impact resistance of the material [15]. Li et al. compared the flexural behaviour of high-performance polypropylene FRALWC and SFRALWC, they found that steel fibres performed better for improving the equivalent initial flexural strength and equivalent residual flexural strength than that of the high-performance polypropylene fibres [16].

The above studies showed that the influences of fibre type on the performance of lightweight aggregate concrete were different. For shale ceramsite lightweight concrete, there were gaps in the study of the mechanical properties of SFRALWC, PFRALWC and BFRALWC that are commonly used in engineering. This study was intended to compare and analyze three types of FRALWC by analyzing compressive strength, splitting tensile strength, energy absorption, high temperature deterioration performance, fracture toughness and dynamic mechanical properties.

The results in this study will provide a basis for the design of FRALWC in a project.

3.Experimental scheme

3.1.Materials and mix proportions

Ordinary Portland cement (C42.5 grade) produced in Jiaozuo Cement Factory was utilized and met the ASTM Type I requirements. Its physical and mechanical properties are shown in Table 1. Fly ash was produced in Jiaozuo Power Plant and met the ASTM Class C requirements. Shale ceramsite (maximum particle size 15 mm) and shale sand were produced in Luoyang Zhengquan Industrial Co., Ltd. The shale ceramsite was 700 grade gravel type with a cylinder compressive strength of 3.2 MPa, a bulk density of 650 kg/m3, and a water absorption of 4.0% at 24 h. The shale sand was 900 grade gravel type with a bulk density of 880 kg/m^3, a water absorption of 12.5% at 24 h, and a fineness modulus of 3.15, which was continuous gradation. The water reducing agent was from the naphthalene series, with a water reducing rate of 15%, and the dosage was 1.6% of the cementing material. The physical and mechanical properties of PPF, wavy SF and chopped BF are shown in Table 2.

Table 1

Physical and mechanical properties of the cement

Setting time (min)		Specific surface area (m^2/kg)	Loss on ignition (%)	SO_3 (%)	Compressive strength (MPa)	
Initial set	Final set				3 d	28 d
127	184	403	2.42	2.61	15.3	46.8

Table 2

Index of the physical and mechanical properties of the different fibres

Type	Density (kg/m^3)	Length (mm)	Diameter (mm)	Elastic modulus (GPa)
PPF	0.91	19	0.048	>3.5
SF	7.80	20	0.500	200
BF	2.65	18	0.015	93-115

Table 3

Mix proportions of the FALWC and ALWC

Code	Material of ALWC					SF (%)	PPF (kg/m^3)	BF (%)
	Cement (kg/m^3)	Fly ash (kg/m^3)	Shale ceramsite (kg/m^3)	Shale sand (kg/m^3)	Water (kg/m^3)			
10	481	157	444	408	171	0	0	0
2P							0.9	
3B								0.2
4S						1.0		

Based on the principle of economy and engineering practicability, the basis mix proportions of LC30 ALWC and the optimum fibre content were determined by using the orthogonal test method and formulated according to the pumping requirements. The mix proportions are shown in Table 3. Code 10 indicates stranded ALWC, Code 2P indicates stranded PFRALWC with an optimum fibre content of 0.9 kg/m^3, Code 3B indicates stranded BFRALWC with an optimal fibre content of 0.2%, and Code 4S indicates stranded SFRALWC with an optimum fibre content of 1%.

3.2.Specimen preparation and test program

ALWC and FRALWC were prepared according to Table 2. Firstly, the shale ceramsite was pre-wetted for 24 hours, mixed with the shale sand and stirred for 1.0 min while adding half of the amount of water evenly. Then, the cement, fly ash and water reducing agent were added gradually and stirred for 3.0 minutes. Finally the fibres and the remaining water were added continuously and stirred for 2.0 min. The concrete was loaded into the mould and demoulded after 24 h. The specimens were cured in a standard curing room with a constant temperature of 20 °C. Compressive strength, energy absorption, high temperature deterioration performance, fracture toughness and dynamic mechanical properties were tested after 28 days, and split tensile strength tests were carried out at 1, 3, 7, 14, and 28 d, respectively. Standard specimens of different sizes were selected according to the type of test, and the cube specimens were used for the compression and split tensile tests. The size of the three-point bending beam specimen was 100 mm × 100 mm × 515 mm. The specimens for the SHPB impact tests were prepared from precast concrete test pieces by core drilling, cutting and grinding. The specified size was Φ50 mm × 25 mm, and the two end faces were required to be parallel.

Compressive strength tests were carried out using a SYE-2000 pressure tester at a rate of 3.0 kN/s according to GB/T50080-2002 (China Industrial Standards). A SYE-300 pressure tester was used to determine the splitting tensile strength of the specimens with a loading rate of 0.5-1.0 kN/s. The experimental equipment is shown in Fig. 1. High temperature tests used a TDL-1400F box type high temperature furnace produced in Beijing Dezhirongtai Environmental Protection Technology Co., Ltd., and the heating rate was 15 °C/min. After reaching the predetermined temperature, the temperature was held constant for 6 h so that the temperatures inside and outside the specimens were equal. Then, the specimens were removed and measured for the compressive strength after these specimens were naturally cooled to room temperature.

The three-point bending notched beam fracture test was carried out per DL/T5332-2005 (China Industrial Standards), and a photo of the experimental beam is shown in Fig. 2. The width of

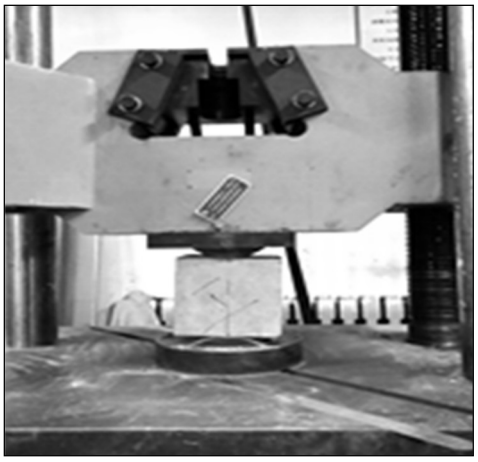

Fig. 1 - The equipment for splitting tensile test.

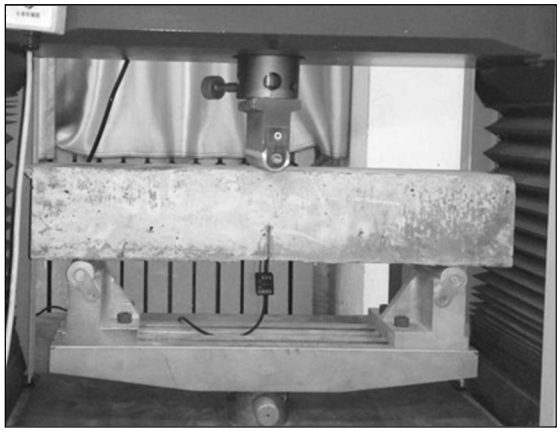

Fig. 2 - The three-point bending beam specimen.

$$K_{IC} = \frac{P_{\max} S}{bh^{\frac{3}{2}}} f[a_0 / h] \quad (1)$$

$$f[a_0/h] = 2.9[a_0/h]^{\frac{1}{2}} - 4.6[a_0/h]^{\frac{3}{2}} + 21.8[a_0/h]^{\frac{5}{2}} - 37.6[a_0/h]^{\frac{7}{2}} + 38.7[a_0/h]^{\frac{9}{2}} \quad (2)$$

where b is the width of the specimen and h is the height of the specimen.

the notch was 3.0 mm. The depth of the notch was 40 mm, recorded as a_0. The mid-span distance of the beam was 400 mm, recorded as S, and the crack length a_0/h was 0.4. According to the maximum load P_{max}, measured by the test, the fracture toughness was calculated according to Eq. (1) recommended by the American Society for Testing Materials (ASTM).

An SHPB impact test system with a variable cross-section was used, and it was powered by compressed nitrogen. The speed of the bullet and the incident bar were controlled via the gas pressure. The bullet impacted the incident bar to generate a one-dimensional stress wave, which acted on the specimen to produce high strain rate deformation. The bullet, incident bar, and transmission bar were all steel rods with a wave velocities C_{so} of 5.19 km/s, densities ρ_s of 7800 kg/m^3, and elastic moduli E_s of 210 GPa. The size of the bullet was Φ50 mm × 1200 mm. Both the incident bar and transmission bar had variable cross-sections with a large-end face diameter of Φ50 mm and a small-end face diameter of 37 mm.

According to the theory of one-dimensional stress waves and stress uniformity, the calculation methods of the average strain rate $\dot{\varepsilon}$, strain ε, and stress σ values of the concrete specimens are shown in Eqs. (3) to (5), respectively.

$$\dot{\varepsilon}(t) = \frac{C_s}{l_{c0}}(\varepsilon_I - \varepsilon_R - \varepsilon_T) \quad (3)$$

$$\varepsilon(t) = \frac{C_s}{l_{c0}} \int_0^{l_{co}} (\varepsilon_I - \varepsilon_R - \varepsilon_T) dt \quad (4)$$

$$\sigma(t) = \frac{A_s}{2A_{c0}} E_s (\varepsilon_I + \varepsilon_R + \varepsilon_T) \quad (5)$$

where A_{c0} and l_{c0} are the initial cross-sectional area and length of the concrete specimen, respectively. E_s, C_s, and A_s are the elastic modulus, wave velocity, and cross-sectional area of the steel bar, respectively. t is the time during which the pulse signal propagated through the concrete specimen. ε_I, ε_R and ε_T are the strain of the incident wave, reflected wave, and transmitted wave, respectively.

In the SHPB test, the energy carried by the incident wave, reflected waves and transmitted wave from the start of loading to the unloading process can be expressed as follows.

$$W_I = A_{C0} E_S C_S \int \varepsilon_I^{\,2}(t) dt \quad (6)$$

$$W_R = A_{C0} E_S C_S \int \varepsilon_R^{\,2}(t) dt \quad (7)$$

$$W_T = A_{C0} E_S C_S \int \varepsilon_T^{\,2}(t) dt \quad (8)$$

Lubricating oil was evenly applied to both end faces of the specimen during the test so that the energy consumed by friction between the specimen and the pressure bar could be ignored. According to the law of conservation of energy, the energy absorbed by the specimen during the impact crushing process can be calculated by Eq. (9).

$$W_A = W_I - W_R - W_T \quad (9)$$

The absorbed energy of the concrete specimen mainly included the crushing energy, the ejection kinetic energy, and the energy dissipated by other forms, such as heat energy, sound energy, and electromagnetic energy. In the rough case, the crushing energy could be used to replace the absorbed energy.

4.Results and discussion

4.1.Compressive strength and specific strength

The compressive strength and specific strength values of FRALWC and ALWC are shown in Fig. 3.

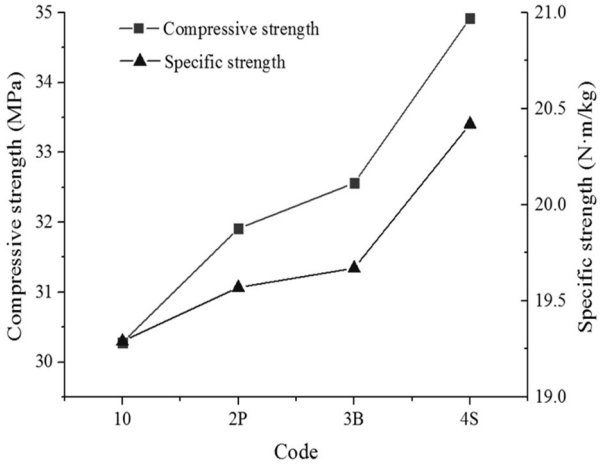

Fig. 3 - Strength of FRALWC and ALWC.

The results showed that the ability of fibres to improve the compressive strength of the ALWC was limited, among which SFALWC had the highest compressive strength, and BF and PPF had no obvious effect on the ALWC compressive strength. This is because the SF has higher rigidity

and a higher elastic modulus. As the specimens being compressed, the SF cooperated with the concrete to resist deformation and improve the compressive strength of the specimens. However, the elastic modulus of BF and PPF were low. When the specimens were compressed, their resistance to deformation were poor, and their contribution to the compressive strength of the specimens were low. In addition, during the preparation of the specimens, the PPF fibres were prone to agglomeration and uneven mixing with the aggregates, resulting in the formation of internal pores. As being subjected to pressure, these pores formed stress concentration areas and accelerated the destruction of the fibre concrete.

To meet the strength requirements, a small cross section was made to reduce self-weight of the structure. The high-quality structural materials should had a high specific strength. The higher the specific strength, the lighter the material used to achieve the corresponding strength. Fig. 3 showed that the specific strength of FRALWC was slightly higher than that of ALWC. SFRALWC had the largest specific strength, and the specific strength of BFRALWC and PFRALWC were approximately equal.

Based on the correlation between compressive strength and specific strength in Fig. 3, the specimen with higher compressive strength had higher specific strength, and a formula was fit out to evaluate the specific strength values of different FRALWC/ALWC. The correlation was shown in Fig. 4, and the relationship could be expressed by a quadratic polynomial with high reliability. As compressive strength grew, specific strength grew faster.

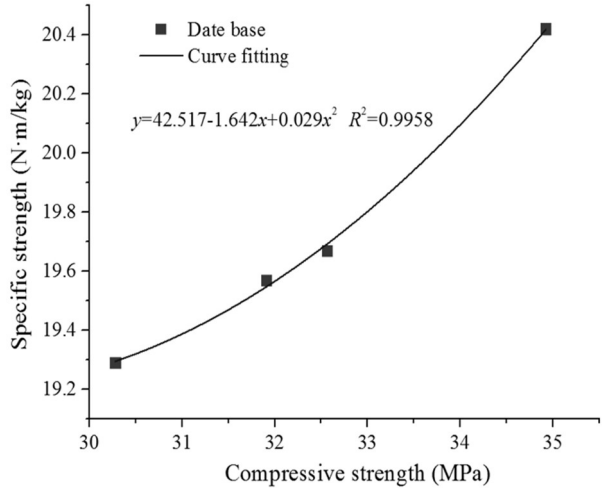

Fig. 4 - Relations between compressive and specific strength.

4.2.Splitting tensile strength

The splitting tensile strength of FRALWC and ALWC at different ages were shown in Fig. 5. The results showed that the splitting tensile strength increased with increasing age and that the rate was faster prior to 7 days. The increasing rate

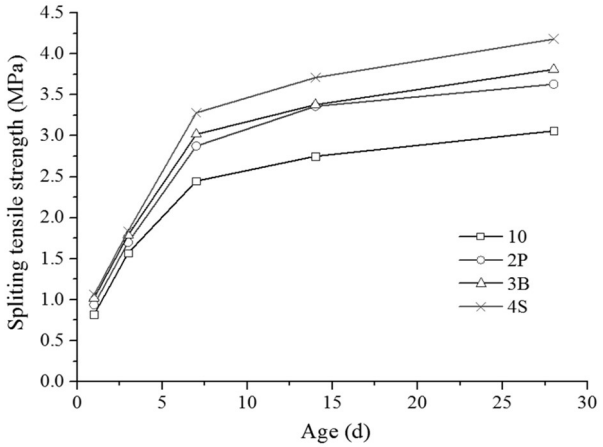

Fig. 5 - Splitting tensile strength growth curves of FRALWC and ALWC.

slowed after 7 days, and the fibres significantly improved the splitting tensile strength of the lightweight concrete. The reason for this phenomenon was that when a specimen was subjected to cracking, the bridging action of the fibres prevented the development of cracks, resisted the continuation of the deformation, and fully utilized the strength-enhancing effect of the fibres. At 28 d, the compressive strength of SFRALWC, PFRALWC and BFRALWC increased by 36%, 19% and 24%, respectively, compared with ALWC without fibres. The effect of SFs was the most obvious, followed by BFs. The effect of PPFs was the smallest.

4.3.Energy absorption

The stress-strain curves of FRALWC and ALWC under quasi-static uniaxial compressive condition were shown in Fig. 6. In the elastic deformation stage, the curves of FRALWC and ALWC were similar. When the peak stress was reached, ALWC showed obvious brittleness, while FRALWC had a plastic plateau. As the post-peak stress decreased by some degrees, the material gradually lost its load carrying capacity and was destroyed. The 70% peak stress was taken as the post-peak stress reduction point, and the corresponding stress-strain integral area was used to represent the material energy absorption index.

As shown in Fig. 7, the energy absorption indices of ALWC, SFRALWC, PFRALWC and BFRALWC were 65.21, 123.78, 95.91, and 109.21 kJ/m^3, respectively. The results showed that the fibres could improve the brittle fracture property of ALWC, increased its plasticity, and improved its energy absorption characteristics. The effect of SF was the most obvious, followed by BF, and PPF had the least influence.

Comparing compressive strength and energy absorption indices of ALWC and FRALWC, it could be found that the specimen with higher compressive strength had higher energy absorption index. As shown in Fig. 8, the relationship between compressive strength and

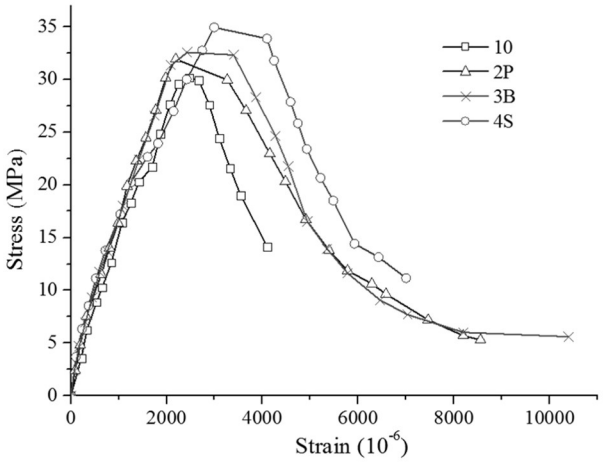

Fig. 6 - Stress-strain curves of FRALWC and ALWC.

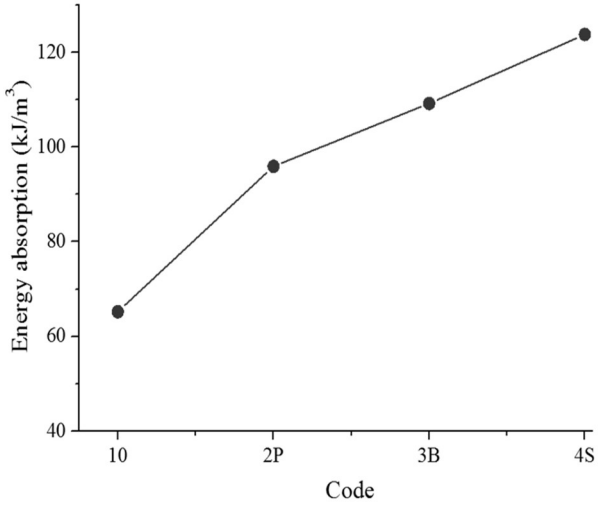

Fig. 7 - Energy absorption indices of FRALWC and ALWC.

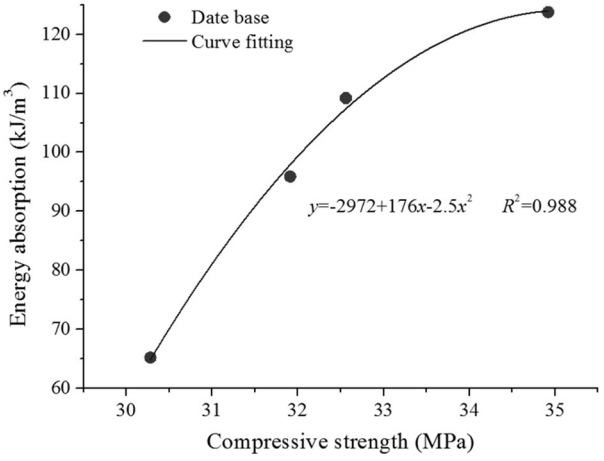

Fig 8 - Relations between compressive strength and energy absorption indices.

energy absorption index could be expressed by a quadratic polynomial with high reliability. With the compressive strength increasing, the energy absorption index also increased.

4.4.High temperature deterioration performance

In the high temperature tests, as being heated to 400 °C, some ALWC specimens burst, and being heated to 450 °C, the remaining specimens burst. After reaching a temperature of 650 °C, some of the BFRALWC and SFRALWC specimens burst, and when the temperature reached 700 °C, the remaining specimens burst. However, no ruptures occurred when the PFALWC specimens were heated to 800 °C. The reason was the melting points of SF and BF were higher, and the disorderly distributed fibres formed a multi-directional restraint system, which improved the bursting resistance of the fibre reinforced lightweight concrete. The melting point of PPF was only 170 °C. When the temperature increased, the melted PPF provided a release channel for the expansion gasses of the chemical decomposition of the lightweight concrete to suppress the occurrence of high temperature bursting.

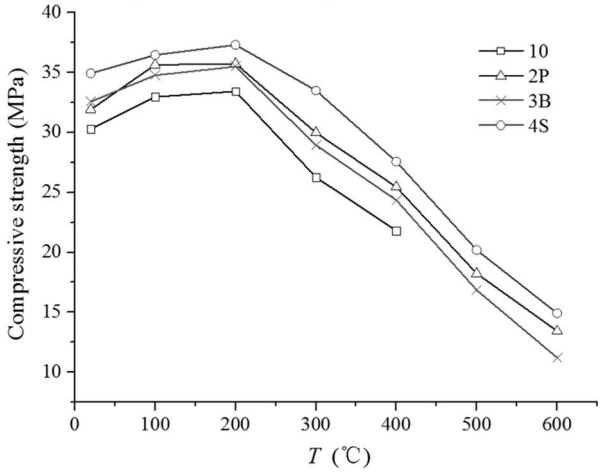

Fig. 9 - The residual compressive strength of FRALWC and ALWC at different temperatures.

The residual compressive strength of the specimens after heating to 20 °C, 100 °C, 200 °C, 300 °C, 400 °C, 500 °C, and 600 °C were shown in Fig. 9. The results showed that the residual compressive strength of the four lightweight concretes were basically the same, and they slowly increased below 200 °C and gradually decreased above 200 °C. This was that below 200 °C, the free water and gel water in the concrete gradually evaporated, forming an environment similar to high-temperature steam curing, so the cement particles were further hydrated, and the strength increased, which was consistent with the literature [17-20]. When the temperature exceeded 200 °C, the internal dehydration of the concrete was intensified, the cement mortar shrunk, cracks appeared on the concrete surface, and the strength decreased [21]. At 400 °C, the residual compressive strength of ALWC, PFRALWC, BFRALWC, and SFRALWC were 67.28%, 73.25%, 78.99%, and 79.11% of their compressive strengths at room temperature, respectively, indicating that the fibres could improve the high temperature resistance to deterioration of ALWC. The effects of SF and BF were the most obvious, followed by PPF.

4.5.Fracture toughness

The load-deflection curves of the three-point bending beam tests of the FRALWC and ALWC specimens were shown in Fig. 10. After reaching the peak values, the loads of the ALWC, SFRALWC and BFRALWC beams fell immediately, lost bearing capacity and showed brittle fracture characteristics. SFRALWC had a high peak load, and its residual strength was maintained at a certain level for a long period of time, showing hardening characteristics. The fracture toughness of FRALWC was shown in Fig. 11. Compared with ALWC, the fracture toughness growth rates of SFALWC and PFALWC were 47% and 8%, respectively, while the BFALWC fracture toughness changed little.

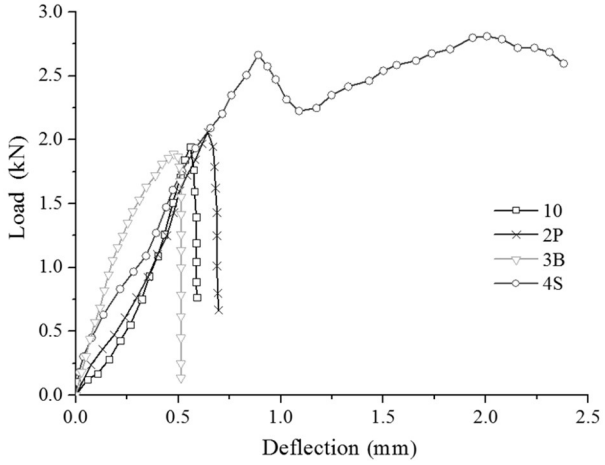

Fig. 10 - Load-deflection curves of FRALWC and ALWC

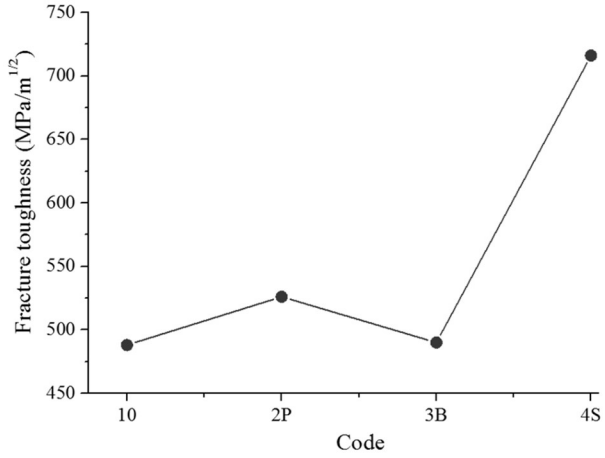

Fig. 11 - Fracture toughness of FRALWC and ALWC

4.6.Dynamic mechanical properties

The specimens were subjected to SHPB dynamic impacts of 0.3 MPa, and the dynamic impact damage patterns were shown in Fig. 12. After the dynamic impact tests, the damage to the ALWC was more serious, with many fragments, and side fragments popped up during the impacts. The PFRALWC and BFRALWC specimens were slightly less damaged, mostly sustaining axially through-type bulk fractures. SFRALWC had the highest degree of integrity after the impacts, and the degree of damage was minimal, with fragmentation only occurring at the edges of the specimens.

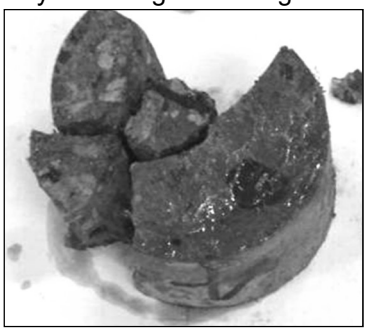

(a) ALWC

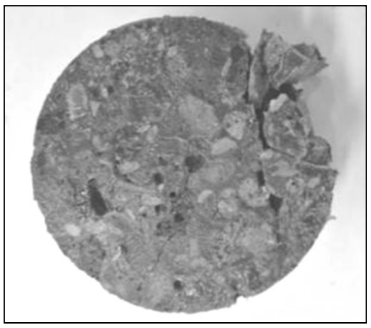

(b) SFALWC

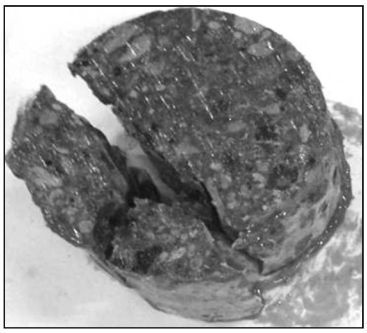

(c) PFALWC

(d) BFALWC

Fig. 12 - Dynamic impact damage pattern of FRALWC and ALWC.

These test results showed that the fibres could effectively improve the failure mode of ALWC under impacts and that a multi-directional restraint system was formed by the disordered distribution of fibres, which prevented the lateral debris of the specimens from being ejected and kept the ALWC failure morphology relatively intact. Compared with PFRALWC and BFRALWC, SFRALWC was more resistant to impact.

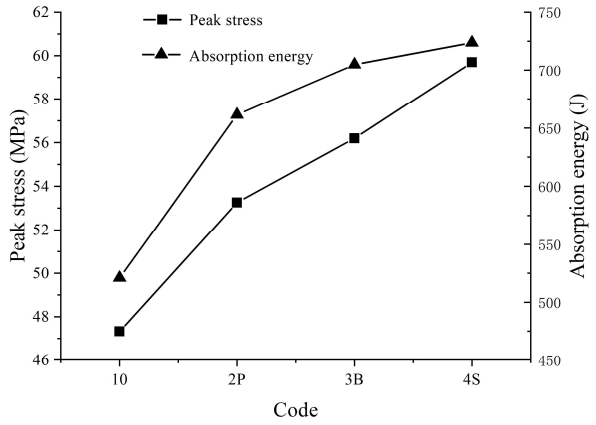

Fig. 13 - Dynamic peak stress and absorption energy for different Codes.

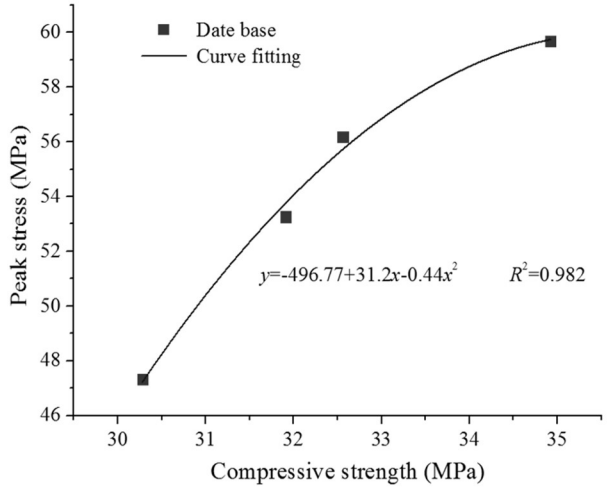

Fig. 14 - Curve of compressive strength and dynamic peak stress.

The pressure of the SHPB dynamic impact tests was set at 0.3 MPa, and the dynamic peak stress and absorption energy of ALWC and FRALWC are shown in Fig. 13. Under similar strain rate conditions, the dynamic peak stress of all samples increased compared with their quasi-static compressive strength, showing the strain rate effect. The dynamic strength growth coefficient, *k*, was defined as the ratio of the dynamic peak stress to the quasi-static compressive strength of the corresponding material. The *k* values of the 10, 2S, 3P, and 4B samples were 1.56, 1.71, 1.67, and 1.73, respectively, indicating that the ability of different fibre types to increase the dynamic peak stress of ALWC was different and that BFRALWC had the highest strain rate sensitivity. The absorption energy characteristic of FRALWC was greatly improved than ALWC, and SFRALWC had the biggest energy consumption. For the compressive strength and dynamic peak stress of ALWC and FRALWC, it could be found that the specimen with higher compressive strength had higher dynamic peak stress. As seen form Fig. 14, the relationship between the compressive strength and dynamic peak stress could be expressed by a quadratic polynomial with high reliability. With the compressive strength increasing, the dynamic peak stress also increased.

5.Conclusions

There are differences in the effects of fibre types on the characteristic of lightweight aggregate concrete. To enrich the mechanical properties of ALWC made by shale ceramsite and shale sand and to provide a basis for FRALWC design in engineering, this study conducted a series of tests to compare and analyse the three types of FRALWC with the best fibre dosage through the evaluation of compressive strength, tensile strength, energy absorption, high temperature deterioration performance, flexural toughness and dynamic mechanical properties. The experimental results obtained in this study are summarized as follows:

(1) The specific strength, energy absorption index and dynamic peak stress of shale ALWC/FRALWC were improved with the compressive strength increasing, and the relation exhibited strong correlation characteristics, which could be expressed by quadratic polynomial. As the compressive strength increased, the growth rate of dynamic peak stress and the specific strength increased quickly, but the growth rate of energy absorption index increased slowly.

(2) The ability of fibres to improve the ALWC compressive strength value was limited, among which SFALWC had the highest compressive strength and BF and PPF had no obvious effect on ALWC compressive strength. The splitting tensile strength of ALWC and FRALWC increased with age, and the growth rate was faster prior to 7 days. The fibres could significantly improve the splitting tensile strength of lightweight concrete. The effect of SF was the most obvious, followed by BF. The effect of PPF was the smallest.

(3) The fibres could improve the brittle fracture property of ALWC, increase its plasticity, and improve the energy absorption characteristics. SFRALWC had the most obvious plasticity, the highest fracture toughness and the biggest energy absorption, followed by BFRALWC and PFRALWC. The fibres could change the burst temperature of ALWC and improve the high temperature resistance to deterioration of ALWC, and the effect of SF and BF were the most obvious, followed by PPF.

(4) The fibres could effectively improve the dynamic impact damage pattern of ALWC, prevent the lateral debris of the specimen from being ejected and keep the ALWC failure morphology relatively intact. Compared with PFRALWC and BFRALWC, SFRALWC was more resistant to impact. However, BFRALWC had the highest strain rate sensitivity.

The dynamic and static mechanical

properties of SFRALWC, PFRALWC and BFRALWC were different. This study focused on the mechanical properties of FRALWC for 28 d standard curing at room temperature. Changes to the curing temperature, such as engineering applications of FRALWC in low and high temperature areas, will be the subject of future research on the rules of strength growth and mechanical properties.

ACKNOWLEDGEMENTS

This work was financially supported by the National Natural Science Foundation of China (51774112; 51474188), the Doctoral Fund of Henan Polytechnic University (B2015-67), and the Taihang Scholars Program. All of these funding sources are gratefully appreciated.

REFERENCES

[1] B. Akcay, M. A. Tasdemir, Effects of distribution of lightweight aggregates on internal curing of concrete, Cem Concr Compos, 2010, **32**(8), 611.

[2] X. F. Wang, C. Fang, W. Q. Kuang, D. W. Li, N. X. Han, F. Xing, Experimental study on early cracking sensitivity of lightweight aggregate concrete, Constr Build Mater, 2017, **136**, 173.

[3] C. G. Go, J. R. Tang, J. H. Chi, Fire-resistance property of reinforced lightweight aggregate concrete wall, Constr Build Mater, 2012, **30**, 725.

[4] S. J. Kwon, K. H. Yang, J. H. Mun, Flexural tests on externally post-tensioned lightweight concrete beams, Eng Struct, 2018, **164**, 128-.

[5] L. J. Kong, Y. B. Du, Effect of lightweight aggregate and the interfacial transition zone on the durability of concretebased on grey correlation, Indian J Eng Mater S, 2015, **22**, 111.

[6] Y. G. Tian, S. F. Shi, K. Jia, S. G. Hu, Mechanical and dynamic properties of high strength concrete modified with lightweight aggregates presaturated polymer emulsion, Constr Buld Mater, 2015, **93**(15), 1151.

[7] P. K. Dehdezi, S. Erdem, M. A. Blankson, Physico-mechanical, microstructural and dynamic properties of newly developed artificial fly ash based lightweight aggregate e Rubber concrete composite, Compos Part B Eng, 2015, **79**, 451.

[8] W. M. Zhang, S. H. Chen, Y. Z. Liu, Effect of weight and drop height of hammer on the flexural impact performance of fiber-reinforced concrete, Constr Build Mater, 2017, **140**, 31.

[9] K. W. Liu, Q. Su, P. P. Ni, C. B. Zhou, W. H. Zhao, F. Yue, Evaluation on the dynamic performance of bridge approach backfilled with fibre reinforced lightweight concrete under high-speed train loading, Comput Geotech, 2018, **104**, 42.

[10] X. F. Wang, C. Fang, W. Q. Kuang, D. W. Li, N. X. Han, F. Xing, Experimental study on early cracking sensitivity of lightweight aggregate concrete, Constr Build Mater, 2017, **136**, 173.

[11] K. G. Babu, D. S. Babu, Behaviour of lightweight expanded polystyrene concrete containing silica fume, Cement Concerte Res, 2003, **33**(5), 755.

[12] G. Wang, B. Zhang, Z. Shui, D. Tang, Y. Kong, Experimental study on the performance and microstructure of rubberized lightweight aggregate concrete, Prog Rubber Plast Re, 2011, **28**, 147.

[13] Y. Z. Zhuang, C. Y. Chen, T. Ji, Effect of shale ceramsite type on the tensile creep of lightweight aggregate concrete, Constr Build Mater. 2013, **46**,13.

[14] D. X. Zhang, W. J. Yang, Experimental research on bond behaviors between shale ceramsite lightweight aggregate concrete and bars through pullout tests, J Mater Civil Eng, 2015, **27**(9), 36.

[15] H. T. Wang, L. C. Wang. Experimental study on static and dynamic mechanical properties of steel fiber reinforced lightweight aggregate concrete, Constr Build Mater, 2013, **38**, 1146.

[16] J. J. Li, J. G. Niu, C. J. Wan, X. Q. Liu, Z. Y. Jin, Comparison of flexural property between high performance polypropylene fiber reinforced lightweight aggregate concrete and steel fiber reinforced lightweight aggregate concrete, Constr Build Mater, 2017, **157**, 729.

[17] B. H. Danuta, J. Góra, W. Andrzejuk, G. Łagód, The microstructure-mechanical properties of hybrid fibres-reinforced self-compacting lightweight concrete with perlite aggregate, Mater, 2018, **11**, 1093.

[18] A. Abrishambaf, M. Pimentel, S. Nunes, Influence of fiber orientation on the tensile behaviour of ultra-high performance fibre reinforced cementitious composites, Cement Concrete Res, 2017, **97**, 28.

[19] Z. Q. Zhang, B. Zhang, P. Y. Yan. Hydration and microstructures of concrete containing raw or densified silica fume at different curing temperatures, Constr Build Mater, 2016, **121**, 483.

[20] D. J. Shen, X. D. Wang, D. B. Cheng, J. Y. Zhang, G. Q. Jiang, Effect of internal curing with super absorbent polymers on autogenous shrinkage of concrete at early age, Constr Build Mater, 2016, **106**, 512.

[21] M. S. Khan, H. Abbas, Effect of elevated temperature on the behavior of high volume fly ash concrete, KSCE J Civ Eng, 2015, **19**(6), 1825.

****